Improving predictions of nearshore wave dynamics and coastal impacts using Smooth Particle Hydrodynamic models

Lowe, Ryan J.; Buckley, Mark L.; Altomare, Corrado; Rijnsdorp, Dirk P.; Suzuki, Tomohiro; Bricker, Jeremy

Publication date
2019

Document Version
Accepted author manuscript

Published in
Australasian Coasts and Ports 2019 Conference; Hotel Grand ChancellorHobart; Australia; 10 - 13 September 2019

Citation (APA)
Lowe, R. J., Buckley, M. L., Altomare, C., Rijnsdorp, D. P., Suzuki, T., & Bricker, J. (2019). Improving predictions of nearshore wave dynamics and coastal impacts using Smooth Particle Hydrodynamic models. In *Australasian Coasts and Ports 2019 Conference; Hotel Grand ChancellorHobart; Australia; 10 - 13 September 2019* (pp. 790-796)

Important note
To cite this publication, please use the final published version (if applicable).
Please check the document version above.

Improving predictions of nearshore wave dynamics and coastal impacts using Smooth Particle Hydrodynamic models

Ryan J. Lowe[1], Mark L. Buckley[1], Corrado Altomare[2], Dirk P. Rijnsdorp[1], Tomohiro Suzuki[3], Jeremy Bricker[4]
[1] Oceans Graduate School, The University of Western Australia, Crawley, Australia
email: Ryan.Lowe@uwa.edu.au
[2] Universitat Politècnica de Catalunya – Barcelona Tech., Barcelona, Spain
[3] Flanders Hydraulics Research, Antwerp, Belgium
[4] Delft University of Technology, Delft, Netherlands

Abstract
In this study we assess the capabilities of the mesh-free, Lagrangian particle method (Smooth Particle Hydrodynamics, SPH) method to simulate the detailed hydrodynamic processes generated by both spilling and plunging breaking waves within the surf zone, and present how the approach can be used to predict a broad spectrum of hydrodynamic processes relevant to coastal applications where wave breaking is important. The weakly-compressible SPH code DualSPHysics was applied to simulate wave breaking over two bathymetric profiles (a plane beach and fringing reef) and compared to experimental flume measurements of waves, currents, and mean water levels. We demonstrate how the model can accurately reproduce a broad range of relevant hydrodynamic processes, ranging from the nonlinear evolution of wave shapes across the surfzone, wave setup distributions, mean current profiles and wave runup. We compare the surfzone predictions with results from other classes of wave models, and illustrate some of the advantages of the SPH approach (particularly in resolving the hydrodynamics above the wave trough). Overall, the results reveal how the mesh-free SPH approach can accurately reproduce the detailed wave breaking processes with comparable skill to state-of-the-art mesh-based Computational Fluid Dynamic models, and how it can be used as a valuable tool to develop new physical insight into surf zone processes.

Keywords: surfzone, wave breaking, wave transformation, nearshore zone, Smooth Particle Hydrodynamics, Computational Fluid Dynamics, *DualSPHysics.*

1. Introduction

The accurate prediction of waves in the nearshore zone has historically been hindered by uncertainty in how to most accurately simulate the breaking process (i.e. overturning of the free surface), and in turn, how this causes organized sea-swell waves to drive a broad range of other motions (e.g. ranging from high-frequency surfzone turbulence to slowly-varying mean currents). The accurate description of the full range of nearshore water motions is critical to develop robust predictions of wave-driven coastal impacts, including coastal flooding, erosion and storm damage to coastal infrastructure.

Nearshore wave models can be broadly placed into two main categories: phase-averaged (spectral) and phase-resolving models. Phase-averaged wave models attempt to simulate the stochastic properties of waves, usually based on linear wave theory, with empirical formulations to parameterize the nonlinear physics (e.g. wave breaking dissipation, wave-wave interactions, etc.). Given that phase-averaged models can only provide crude representations of complex surf zone physics, they often require some degree of parameter tuning to match experimental observations. This can undermine their predictive value, especially when applied to sites with limited (or no) data available for validation.

Phase-resolving wave models, loosely defined here as any wave-flow model that deterministically resolve motions at time-scales shorter than individual sea-swell waves, include a more complete representation of the nonlinear physics of nearshore waves. Depth-averaged (2DH, two-dimensional in the horizontal) versions of these models (or multi-layer versions employed with coarse vertical resolution) are commonly based on solution of either the Boussinesq equations or nonlinear shallow water equations with nonhydrostatic pressure corrections. While 2DH phase-resolving models may more accurately simulate the nonlinear behaviour of non-breaking waves compared to phase-averaged models, they are still incapable of directly resolving the wave breaking process and thus often also require significant parameterization of the breaking process.

Three-dimensional (3D) phase-resolving wave-flow models provide the most rigorous representation of nearshore hydrodynamics, including the capability to directly resolve at least some wave breaking process, but are computationally expensive. Traditionally these models have been solved on fixed meshes (grids) based on various solutions of Eulerian forms of the (Reynolds-Averaged) Navier-Stokes equations. This includes multi-layered non-hydrostatic wave-flow models [e.g., 1, 2, 3], as well as more computationally demanding Computational Fluid Dynamic (CFD) models such

OpenFOAM [e.g., 4, 5]. Of these model types, only the latter (CFD models) are able to directly resolve the overturning free surface characteristics of breaking waves.

More recently, a number of mesh-free CFD modelling approaches have also been developed based on Lagrangian solution of the Navier-Stokes equations, including those based on the Smoothed Particle Hydrodynamics (SPH) approach. SPH has become an increasingly common technique applied to coastal engineering problems, due to its ability to deal with complex geometries and to simulate large deformations at interfaces (including moving boundaries and at the free surface) [e.g., 6, 7-13]. Nevertheless, despite the great promise of SPH for coastal applications, rigorous assessment of the capabilities of SPH models to accurately simulate a full range of relevant surf zone hydrodynamic processes is still relatively sparse, certainly in comparison to the wealth of information derived from detailed nearshore wave modelling studies (including mesh-based CFD modelling approaches).

In this study, we conduct a detailed assessment of the ability of SPH models to predict a broad range of nearshore hydrodynamic processes relevant to coastal applications where wave breaking is important. Using experimental data of wave breaking over both a plane beach and a fringing reef profile, we demonstrate how the model can accurately reproduce a broad range of relevant hydrodynamic processes, ranging from the nonlinear evolution of wave shapes across the surf zone, wave setup distributions, mean current profiles and wave runup. We compare the surf zone predictions with predictions by other classes of wave models from literature, and illustrate some of the advantages of the SPH approach (particularly in resolving hydrodynamics above the wave trough).

2. Methodology

2.1 Background on the SPH approach

Smoothed Particle Hydrodynamics (SPH) is a mesh-less numerical method where a continuum is discretized into particles. The approach was originally developed within astrophysics [14] and has since been largely applied across a wide range of Computational Fluid Dynamics (CFD) applications. Within SPH the particles represent calculation nodal points that are free to move in space according to the governing Lagrangian dynamics, e.g. in fluid mechanics based on the Navier-Stokes equations [15]. The kinematic and dynamic properties of each particle (e.g., position, velocity, density pressure, etc.) then result from the interpolation of the values of the neighbouring particles by application of a weighted kernel function (W) that is defined over a characteristic smoothing length h_{SPH}. The mathematical foundation of SPH is thus based around integral interpolants, in which any function $F(\vec{r})$ in coordinate space $\vec{r}$ can be computed by the integral approximation:

$$F(\vec{r}) = \int F(\vec{r}')\, W(\vec{r} - \vec{r}', h_{SPH}) d\vec{r}' \qquad (1)$$

that can also be expressed in a discrete form based on particles. The momentum equation in discrete SPH form for a weakly compressible fluid then can be written following Monaghan [15] as:

$$\frac{d\vec{u}_a}{dt} = -\sum_b m_b \left(\frac{P_b + P_a}{\rho_b \rho_a} + \Pi_{ab}\right) \nabla_a W_{ab} + \vec{g} \qquad (2)$$

where t is time, $\vec{u}_a = \frac{d\vec{r}_a}{dt}$ is velocity of particle a, P is pressure, $\vec{g}$ is gravitational acceleration, W_{ab} is the kernel function that depends on the distance between particles a and b. The effect of viscous dissipation within SPH can be approximated using the artificial viscosity term Π_{ab} [15], as well as various Sub-Particle Scale (SPS) turbulence closure models [16, 17]. In the present study, we use the artificial viscosity formulation that relates velocity gradients in the flow to viscous stresses using an artificial viscosity coefficient α that produces the effect of a shear and bulk viscosity.

In a similar way, a discrete form of the continuity equation can be expressed as:

$$\frac{d\rho_a}{dt} = \sum_b m_b \left(\vec{u}_a - \vec{u}_b\right) \cdot \nabla_a W_{ab} \qquad (3)$$

For weakly-compressible SPH (used in this study), pressure and density are explicitly-related by Tait's equation of state, which allows the approach to be readily parallelized in numerical codes, given that the motion of each particle can be solved independently (explicitly), including on Graphics Processing Units (GPUs).

The present study uses the open-source solver DualSPHysics (http://dual.sphysics.org/) based on WCSPH [18, 19]. DualSPHysics is written in two languages, namely C++ and CUDA, and optimized to use the parallel processing power of either CPUs and/or GPUs [20]. For wave generation, DualSPHysics implements different schemes. In the present study, waves were generated using boundary particles as moving boundaries that mimic the movement of a wavemaker in a physical facility [21].

2.2 Experimental cases

Model performance was assessed using observations from two experimental datasets that include a range of regular (monochromatic) wave conditions and bathymetry profiles. The two

experimental datasets comprise (Figure 1): 1) the two test cases of regular wave breaking on a plane beach described in Ting and Kirby [22] (hereafter denoted TK94) that include both 'spilling' and 'plunging' wave breaking conditions; and 2) the two test cases described in Yao [23] (hereafter Y12) that report regular wave transformation across a reef profile at two water depths.

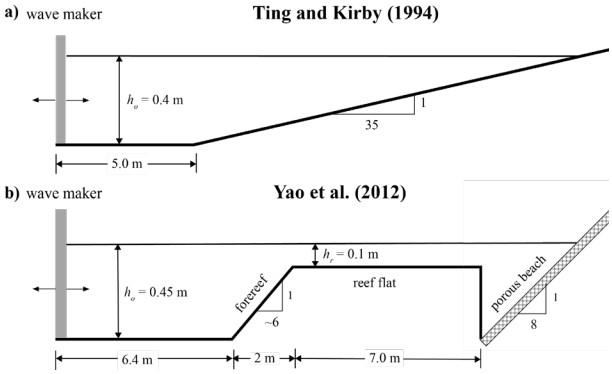

Figure 1 Experimental setup as simulated in the model for the (a) Ting and Kirby (1994) [22] and (b) Yao et al. (2012) [23] test cases. In both cases, the flat offshore region was shortened for computational efficiency. The Yao et al. (2012) case is specifically drawn for Case 1 where hr=0.1 m. Note that vertical scale is exaggerated by 8:1.

2.2.1 Plane beach - Ting and Kirby (1994)

TK94 obtained detailed measurements of the mean and turbulent flow structures generated by regular wave breaking on a linear-sloping plane beach (note that subsequent analysis of this dataset is also described in Ting and Kirby [24] and Ting and Kirby [25]). The wave flume was configured with an initial flat bed (depth h=0.4 m) followed by a beach with 1:35 slope (Figure 1a). 'Spilling' breaking waves were generated by incident waves with offshore wave height H=0.125 m and period T=2.0 s; whereas 'plunging' breaking waves were generated by waves of effectively the same height at breaking (H=0.128 m) but with longer period (T=5 s). For both cases, water elevations (η) were recorded using capacitance wave gauges at ~20 cross-shore locations; whereas, vertical profiles of current velocities (both horizontal u and vertical w velocity components) were obtained using laser Doppler anemometry at several cross-shore locations (8 and 7 locations for the spilling and plunging cases, respectively).

2.2.2 Fringing reef – Yao et al. (2012)

Y12 describe measurements of wave transformation across a reef profile with a steep (~1:6) sloping forereef and 7 m wide horizontal reef flat located 0.35 m above the wave flume bottom (Figure 1b). At the back of the reef flat, the depth extended again to the bottom of the flume and was followed by a 1:8 beach covered with a porous mat to dissipate wave energy. We focus here on two of the test cases described in Y12 (denoted Case 1 and 3 in that study), which used similar regular wave conditions (incident wave heights of H=0.095 m and H=0.101 m, and periods T=1.25 s and 1.00 s for Cases 1 and 3, respectively). The main difference between cases was the still water level relative to the reef flat: Case 1 had a still-water reef flat depth of h_r=0.1 m, whereas for Case 3 the still water level was at the reef flat level (i.e. h_r=0 m). For both cases, water levels were measured at 12 locations.

2.3 Model settings and post-processing

The numerical simulations were conducted using version 4.2 of DualSPHysics in a 2DV (vertical) plane. To provide a rigorous and transparent assessment of model performance over the range of test cases, we concentrated on using default or typical model parameter settings reported in the literature that were held constant across all numerical results reported here, i.e. we did not vary parameters across different test cases to optimize performance.

For all simulations we used an initial inter-particle spacing dp=2 mm to balance model performance with computational expense (both when running simulations and post-processing large volumes of model output). This translated to simulating ~1.22 million particles in both TK94 test cases, and ~1.24 million and ~830 thousand particles for Case 1 and 3 of Y12, respectively. Note that the smoothing length h_{SPH} defined in section that governs the size of the kernel that determines particle-particle interactions in SPH is related to dp as $h_{SPH} = coef h\sqrt{2}dp$, where $coefh$ is a smoothing coefficient of order 1 that determines the scale of interactions with adjacent particles. In all simulations we used $coefh$ = 1.2, which given dp=2 mm implies an effective smoothing length of h_{SPH}~3 mm.

A wide range of studies have investigated the optimal value of α in numerical wave flume studies and have consistently found this to be of order 0.01 [e.g., 21, 26, 27]. We likewise found that model performance was optimal over a range of α =0.005-0.05 (not shown), and thus chose to use a default value for the artificial viscosity coefficient (α =0.01) that has been recommended for coastal applications [21, 27], which was held constant across all runs.

All numerical simulations were conducted at the Pawsey Supercomputing Centre in Perth, Australia on supercomputer (Zeus) with GPU-capable nodes. Each run simulated 360 seconds of experimental time, which corresponded to a minimum of ~100 waves that ensured convergence of the mean and turbulent flow characteristics. To compare the simulation results to the fixed (Eulerian) experimental measurements, for an array of points specified on a grid, a kernel function

(averaging length $2h_{SPH}$) was used to interpolate the individual SPH particle properties to the grid.

Time series of the model output (water levels and velocities) were decomposed into mean and wave contributions by ensemble averaging over the periodic waves.

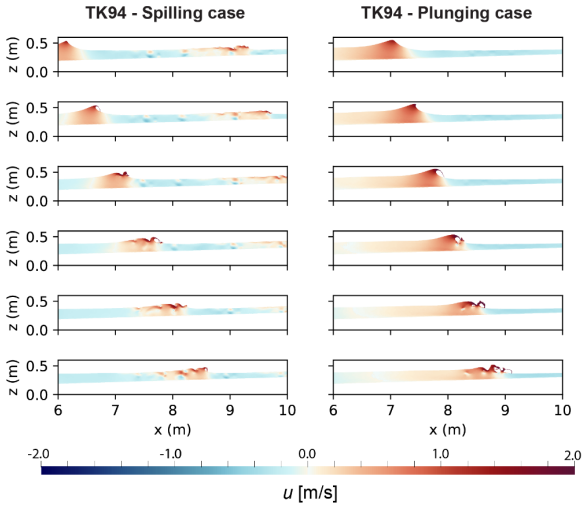

Figure 2 Evolution of wave breaking on a plane beach from TK94 with colours denoting the horizontal (u) velocity component (reds onshore, blues offshore). (Left) spilling case. (Right) plunging case. Note that the velocity output is at 0.2 s interval.

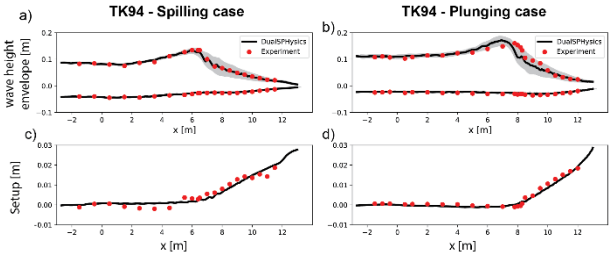

Figure 3 Wave height envelope and wave setup evolution for the (Left column) spilling wave case and (Right column) plunging wave case in TK94. (Top row) envelope of the maximum crest and minimum trough wave elevation. (Bottom row) Wave setup. Grey regions denote one standard deviation of the water elevations from the ensemble (wave) average.

3. Results

The results presented below specifically focus on results for the TK94 experiments of wave breaking over a plane beach to highlight the model performance. The Y12 experiments were simulated with comparable model skill (not shown) and will be left for future presentation.

Although both of the TK94 test cases had breaking wave heights that were approximately the same, the difference in wave period resulted in appreciable differences in how waves broke and transformed within the surf zone (Figure 2). For both of the test cases, the cross-shore variations in wave heights were accurately predicted by the model, as illustrated here by comparison of the ensemble-averaged crest (η_{max}) and trough locations (η_{min}) (Figure 3). Small discrepancies tend to fall within the variability among individual waves. The cross-shore variations in wave setup ($\overline{\eta}$) were also well-predicted by the model (Figure 3).

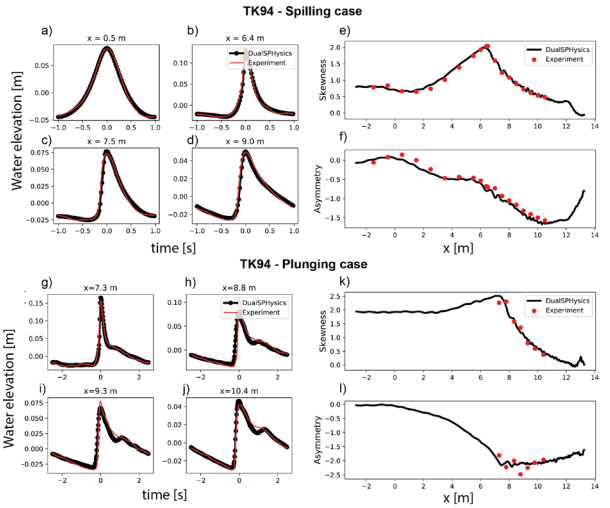

Figure 4 Water surface elevation (wave ensemble-averaged) and wave shape (skewness and asymmetry evolution for TK94. (Top set of panels) Spilling case. (Bottom set of panels) Plunging case. Note that t=0 s is referenced to the time of maximum water level at a given location.

Figure 4 shows the wave water level timeseries ($\tilde{\eta}$), which are ensemble-averaged over a wave period, as well as the skewness (Sk) and asymmetry (As) parameters that characterize nonlinear wave shape. For the four example locations shown, which span the shoaling, outer surf zone, and inner surf zone regions, the wave phase-averaged water level timeseries agree well with the observations. This includes the more complex wave shapes for the plunging case, where there is very rapid rise of the free surface just prior to the arrival of the crest, followed by the much slower fall of the free surface that includes an inflection (small second local maximum) in the water level. While this inflection is slightly more pronounced in the observation, its occurrence and timing are still predicted by the model. The close agreement between the modelled and observed wave skewness and asymmetry is particularly remarkable, given this covers a large number of measurement locations and wave states as they transform from deep water to the shoreline and given that as third-order bulk statistical parameters of the waves are generally more difficult to predict relative to wave heights.

The mean Eulerian current profiles show distinct reversals in flow above and below the mean wave trough elevation consistent with an expected undertow profile, with onshore flow within the crest region and offshore flow below the trough (Figure 5). The modelled mean current profiles are generally in good agreement with the observations. Above the trough, the model compares reasonably well in the lower portion of the region where measurements could be made; further above this elevation (where no observations are available), the model predicts a local maximum in each current profile with the velocity then decreasing again towards the crest. For the region below the trough, for the spilling case the model tends to accurately predict the shape and magnitude of the undertow profile; however, at some locations shoreward of the breakpoint, the model tends to predict a slightly more vertically-sheared profile. For the plunging case, the undertow within the inner surf zone is accurately predicted; however, similar to the spilling case, within the outer surf zone immediately seaward of the breakpoint, there is more vertical shear in the undertow profile than observed and overall there is excess flow directed offshore.

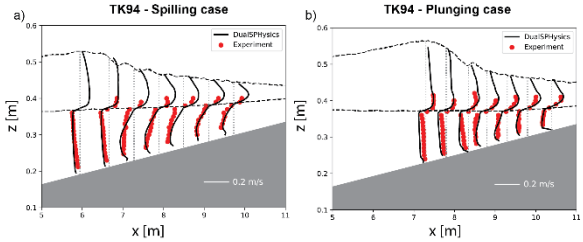

Figure 5 Cross-shore horizontal mean current (u) profiles for the a) spilling and b) plunging wave cases in TK94. The horizontal dashed lines denote the ensemble averaged crest and trough elevations. Vertical dotted lines coincide with u=0.

4. Discussion and conclusions

This study has demonstrated how the mesh-free SPH approach can provide accurate and robust predictions of surf zone hydrodynamic processes generated by wave breaking, with model performance comparable to applications state-of-the-art mesh-based CFD models such as OpenFOAM. Over the wide range of wave breaking types considered, the SPH approach was able to reproduce many of the detailed processes that govern the nonlinear evolution of wave shape in the nearshore, the free surface characteristics of breaking waves (including violent, plunging waves), the processes governing wave energy conversion between potential and kinetic energy within the surf zone, and resulting mean wave-driven flow properties (including wave setup and undertow profiles). A particular advantage of approach used here (the weakly-compressible SPH code DualSPHysics), was its ability to run on computationally-efficient GPUs that enabled high-resolution simulations (sub-millimeter particle spacing) of the experimental results to be achieved on a single-GPU.

Given that the performance of the SPH approach was evaluated using common experimental test cases (e.g. TK94) that have been widely-applied to benchmark the performance of other classes of phase-resolving wave-flow models (e.g., Boussinesq, non-hydrostatic, and CFD), the results also provide an opportunity to inter-compare how different defining characteristics of these models may influence model performance. Based on prior model applications to these experimental datasets, a wide range of phase-resolving models (including depth-averaged versions) have been found to be fully-capable of accurately resolving the nonlinear evolution individual waves prior to breaking. However, within the surf zone region, where phase-resolving models cannot directly resolve the overturning free surface, more variable model performance has been reported across the literature. By necessity, depth-averaged versions of these models (e.g. based on Boussinesq and non-hydrostatic approaches) require significant empirical parameterization of the breaking process. Therefore, while these models have often been successful in reproducing surf zone wave transformation, they generally require tuning of empirical parameters (generally on a case-by-case basis), which can undermine their broader predictive utility and this tuning may also come at the expense of other hydrodynamic predictions (e.g., degrading that accuracy of wave setup distributions).

Mesh-based 3D/2DV models with vertical resolution (e.g. multi-layer non-hydrostatic and CFD models) have been shown in recent years to provide more robust predictions of surf zone wave transformation, as they depend much less on empirical parameterization of the breaking process. Of these models, CFD models based on full solution of the Reynolds Averaged Navier Stokes equations are most analogous to the present SPH simulations as they both can directly resolve overturning, breaking waves. In the context of recent recent applications of high-resolution mesh-based CFD models (i.e. OpenFOAM) that have been applied to the same experimental test cases [e.g., 4, 5, 28], the present results indicate that the SPH approach can reproduce these surf zone processes with comparable skill. In fact, there are some suggestions that the SPH approach can help to improve predictions within the crest region of breaking waves, e.g. as evident by robust predictions of cross-shore mass fluxes that have been notoriously difficult to predict in mesh-based CFD models. Moreover, considering the broader

context of nearshore wave modelling, arguably the greatest advantage of mesh-free SPH models is how readily they can deal with complex geometries (bathymetry and topography) that may not readily conform to a fixed mesh (grid). Therefore, while both SPH and mesh-based CFD models may be used interchangeably in applications with simple nearshore bathymetries (i.e. as in the test cases considered here), the SPH approach may confer greater advantages when simulating nearshore processes with coastal engineering structures or natural bathymetries that form complex geometries.

While the present study has demonstrated the great promise of the SPH modelling approach to improving understanding and prediction of surf zone hydrodynamics, it is important to acknowledge that the present focus has been on investigating the performance under relatively simple forcing (i.e. regular waves) and simple bathymetry profiles. This approach was deliberately chosen as an initial starting point to help isolate the performance characteristics of SPH models in the simulation of surf zone hydrodynamics using a simple set of wave breaking conditions. This present work should provide a foundation for further SPH modelling studies of surf zone hydrodynamics under more realistic conditions, including irregular wave conditions and for applications to more complicated nearshore bathymetry profiles (e.g. barred beaches, various reef geometries, etc.) where a wealth of experimental data also exists to investigate model performance. While such studies are achievable today, the primary constraint (particularly for irregular wave conditions) is the requirement of much longer simulations (typically more than an order of magnitude greater), and hence computational demand, which is required to properly resolve the statistical properties of irregular waves. For the SPH code used in the present study (DualSPHysics), this greater computational demand can be partially offset by recent developments in coupling the SPH model with efficient phase-resolving wave models [e.g., 8, 29, 30], thereby concentrating the focus of the SPH simulations on the immediate surf zone region; as well as plans for multi-GPU functionality of the code in future code releases.

Finally, with SPH applications to coastal problems still in its early stages (certainly in comparison to decades of work using mesh-based models), the many areas of active research and develop of the SPH approach will help to further advance surf zone applications into the future. This includes many new developments in, for example, improved boundary conditions (solid boundaries and at the free surface), inclusion of multi-phase behaviour, enhanced numerical optimization (including adaptive refinement of particle resolution), and greater accuracy using approaches such as incompressible SPH (ISPH) (e.g. refer to recent reviews by Violeau and Rogers [31] and Gotoh and Khayyer [32]). One area that deserves particular attention in future SPH studies of nearshore wave dynamics is the role of surf zone turbulence, with advanced turbulence models (sub-particle scale) still being an active area of research. The present study can highlight some interesting attributes of the turbulence fields generated by the breaking waves, but only describes those motions that are directly resolved at the particle scale (albeit the simulations were conducted at relatively high resolution). Future dedicated work on surf zone turbulence is needed to better understand how it influences the range of nearshore hydrodynamic processes, including investigating how effectively turbulent motions can be represented using sub-particle scale turbulent closure schemes.

5. Acknowledgements

This work was supported by resources provided by the Pawsey Supercomputing Centre with funding from the Australian Government and the Government of Western Australia. We are grateful to Yao Yu for providing the experimental data to help evaluate the data, as well as the helpful discussions about this modelling with Marion Tissier, Ad Reniers, Ap van Dongeren, Dano Roelvink, Robert McCall, and Niels Jacobsen while RJL was on a sabbatical in Delft, the Netherlands. RJL thanks both Deltares and Delft University of Technology for hosting his time in the Netherlands.

6. References

[1] Zijlema, M. and G.S. Stelling, Efficient computation of surf zone waves using the nonlinear shallow water equations with non-hydrostatic pressure. Coastal Engineering, 2008. 55(10): p. 780-790.

[2] Bradford, S.F., Nonhydrostatic model for surf zone simulation. Journal of Waterway, Port, Coastal, and Ocean Engineering, 2010. 137(4): p. 163-174.

[3] Ma, G., F. Shi, and J.T. Kirby, Shock-capturing non-hydrostatic model for fully dispersive surface wave processes. Ocean Modelling, 2012. 43-44: p. 22-35.

[4] Brown, S.A., et al., Evaluation of turbulence closure models under spilling and plunging breakers in the surf zone. Coastal Engineering, 2016. 114: p. 177-193.

[5] Larsen, B.E. and D.R. Fuhrman, On the over-production of turbulence beneath surface waves in Reynolds-averaged Navier–Stokes models. Journal of Fluid Mechanics, 2018. 853: p. 419-460.

[6] Monaghan, J. and A. Kos, Solitary waves on a Cretan beach. Journal of waterway, port, coastal, and ocean engineering, 1999. 125(3): p. 145-155.

[7] St-Germain, P., et al., Smoothed-particle hydrodynamics numerical modeling of structures

impacted by tsunami bores. Journal of Waterway, Port, Coastal, and Ocean Engineering, 2013. 140(1): p. 66-81.

[8] Altomare, C., et al., Hybridization of the wave propagation model SWASH and the meshfree particle method SPH for real coastal applications. Coastal Engineering Journal, 2015. 57(4): p. 1550024-1-1550024-34.

[9] Crespo, A., et al., Towards simulating floating offshore oscillating water column converters with smoothed particle hydrodynamics. Coastal Engineering, 2017. 126: p. 11-26.

[10] González-Cao, J., et al., On the accuracy of DualSPHysics to assess violent collisions with coastal structures. Computers & Fluids, 2019. 179: p. 604-612.

[11] Zhang, F., et al., DualSPHysics: A numerical tool to simulate real breakwaters. Journal of Hydrodynamics, 2018. 30(1): p. 95-105.

[12] Altomare, C., et al., Numerical modelling of armour block sea breakwater with smoothed particle hydrodynamics. Computers & Structures, 2014. 130: p. 34-45.

[13] Domínguez, J., et al., Towards a more complete tool for coastal engineering: solitary wave generation, propagation and breaking in an SPH-based model. Coastal Engineering Journal, 2019: p. 1-26.

[14] Lucy, L.B., A numerical approach to the testing of the fission hypothesis. The astronomical journal, 1977. 82: p. 1013-1024.

[15] Monaghan, J.J., Smoothed particle hydrodynamics. Annual review of astronomy and astrophysics, 1992. 30(1): p. 543-574.

[16] Gotoh, H., S. Shao, and T. Memita, SPH-LES model for numerical investigation of wave interaction with partially immersed breakwater. Coastal Engineering Journal, 2004. 46(01): p. 39-63.

[17] Dalrymple, R.A. and B. Rogers, Numerical modeling of water waves with the SPH method. Coastal engineering, 2006. 53(2-3): p. 141-147.

[18] Crespo, A.C., et al., GPUs, a new tool of acceleration in CFD: efficiency and reliability on smoothed particle hydrodynamics methods. PloS one, 2011. 6(6): p. e20685.

[19] Crespo, A.J., et al., DualSPHysics: Open-source parallel CFD solver based on Smoothed Particle Hydrodynamics (SPH). Computer Physics Communications, 2015. 187: p. 204-216.

[20] Domínguez, J.M., A.J. Crespo, and M. Gómez-Gesteira, Optimization strategies for CPU and GPU implementations of a smoothed particle hydrodynamics method. Computer Physics Communications, 2013. 184(3): p. 617-627.

[21] Altomare, C., et al., Long-crested wave generation and absorption for SPH-based DualSPHysics model. Coastal Engineering, 2017. 127: p. 37-54.

[22] Ting, F.C. and J.T. Kirby, Observation of undertow and turbulence in a laboratory surf zone. Coastal Engineering, 1994. 24(1-2): p. 51-80.

[23] Yao, Y., et al., 1DH Boussinesq modeling of wave transformation over fringing reefs. Ocean Engineering, 2012. 47: p. 30-42.

[24] Ting, F.C. and J.T. Kirby, Dynamics of surf-zone turbulence in a strong plunging breaker. Coastal Engineering, 1995. 24(3-4): p. 177-204.

[25] Ting, F.C. and J.T. Kirby, Dynamics of surf-zone turbulence in a spilling breaker. Coastal Engineering, 1996. 27(3-4): p. 131-160.

[26] De Padova, D., R.A. Dalrymple, and M. Mossa, Analysis of the artificial viscosity in the smoothed particle hydrodynamics modelling of regular waves. Journal of Hydraulic Research, 2014. 52(6): p. 836-848.

[27] Roselli, R.A.R., et al., Ensuring numerical stability of wave propagation by tuning model parameters using genetic algorithms and response surface methods. Environmental Modelling & Software, 2018. 103: p. 62-73.

[28] Jacobsen, N.G., D.R. Fuhrman, and J. Fredsøe, A wave generation toolbox for the open-source CFD library: OpenFoam®. International Journal for Numerical Methods in Fluids, 2012. 70(9): p. 1073-1088.

[29] Altomare, C., et al., Improved relaxation zone method in SPH-based model for coastal engineering applications. Applied Ocean Research, 2018. 81: p. 15-33.

[30] Verbrugghe, T., et al., Coupling methodology for smoothed particle hydrodynamics modelling of non-linear wave-structure interactions. Coastal Engineering, 2018. 138: p. 184-198.

[31] Violeau, D. and B.D. Rogers, Smoothed particle hydrodynamics (SPH) for free-surface flows: past, present and future. Journal of Hydraulic Research, 2016. 54(1): p. 1-26.

[32] Gotoh, H. and A. Khayyer, On the state-of-the-art of particle methods for coastal and ocean engineering. Coastal Engineering Journal, 2018. 60(1): p. 79-103.